A Method for Automatic Radar Azimuth Calibration using Stationary Targets

Alexandru Bobaru
Communications Dept.
Politehnica University of Timisoara
Timisoara, Romania
corneliu.bobaru@student.upt.ro

Corina Nafornita
Communications Dept.
Politehnica University of Timisoara
Timisoara, Romania
corina.nafornita@upt.ro

Cristian Vesa
Hella Romania
Timisoara, Romania
VladimirCristian.Vesa@hella.com

***Abstract*—Radar is one of the fundamental sensors used in ADAS (Advanced Driver Assist System). Automotive related functionalities like ACC (Adaptive Cruise Control), LCA (Lane Change Alert), CTA (Cross Traffic Alert) or TA (Turn Assist) require very precise detection and ranging of traffic and environment, otherwise, the whole ADAS performance can be degraded. Vehicle integration and mounting tolerances will influence the angular performance of the radar sensor, due to its installation behind a bumper or a cover and even due to aging or exposure to accidents or vehicle vibration. In this paper, we introduce a real time autocalibration method of an azimuth angular interval to correct the environmental influences on the sensor.**

Keywords—Automotive Radar, azimuth calibration, automatic calibration, ADAS

I. INTRODUCTION

In the past decades, the need for driver assistance systems in the automotive industry has increased steadily. The main reason for this is the need for increasing the driver's comfort and safety, with functionalities that play a supporting role in helping the driver and thus, decreasing the number of accidents in public road traffic [1].

That means that an ADAS must contain several systems that would intervene in case of potentially dangerous situations to prevent them as soon as they happen. One such system used is the radar, that has active functionalities like LCA, CTA, or TA, that perform traffic monitoring and assess potential danger of vehicles, releasing a warning for the driver. These functionalities require precise detection and ranging of the environment and traffic. For this purpose, automotive radar systems detect objects and obstacles, known as targets, with corresponding range, azimuth-elevation angles, and velocity. However, the radar systems are usually installed behind painted bumpers or covers, meaning that factors like coating properties, shape, material and paint will lead to a performance degradation in the angle measurement. The measurements are affected by errors from reflections, diffraction, refraction, and multipath propagation of the signal that depend on the angle of the incident wave. These distortions will be referred as local offsets throughout this paper.

There are different methods for compensating such offsets, such as optimizing the vehicle integration by electromagnetic simulations and pre-evaluation of functional behavior, leading to the creation of a specific angle correction characteristic.

These calibration methods have been already studied very well in the literature [2]. To compensate for local angular distortions in the azimuth, there are various offline methods based either on simulations that include knowledge of bumper properties, or on methods that require the reception of a signal from a target with a known angle [1]. For automotive radars, these types of offline calibration present great difficulties due to the need to calibrate the sensors after mounting them behind the bumper, as well as the high cost of allocating a special space for setup and preparing the plant personnel. Due to their effort, these methods can be used only for an initial calibration of a radar sensor.

The correction method should ideally be automatic and adaptive, considering both radar wear and the changes of the bumper properties over the years. A self-calibration method with a target with unknown position allows an initial calibration as well as a continuous adjustment during the lifetime of the sensor. Harter et al. developed a self-calibration model for a MIMO radar [3], but it's difficult to adapt to a SIMO radar. Suzuki et al. [4] proposed a feasible method for different types of radars, which generates a correction table by performing a regression of the bias error function. A disadvantage of this solution is the incorporation of the Gaussian process regression with Monte Carlo Markov Chain (MCMC) method in performing the regression of the error function, due to the intensive computing power required by the stochastic sampling involved. Another method of online self-correction of local angular distortions in azimuth, proposed by Kostka el al. [5] consists in estimating the real trajectory (reference) of a radar object that performs an overtaking maneuver, relative to the ego vehicle. An angle measurement error between the measured angle and the actual angle is determined by evaluating the movement pattern of the object. However, a disadvantage of this solution is represented by the scarcity of the required events that can trigger the correction calculation process.

The requirement is to perform a continuously adjustable and tunable azimuth automatic calibration process which can adapt on any vehicle, can accurately compensate azimuth local offsets in a robust manner and can provide statistical data that characterize the resulting angle correction characteristic in a global manner.

The main contributions of this paper are as follows:

- A fully functional model that can adapt the radar system to the vehicle integration.
- An algorithm that provides continuous corrections based on stationary targets and references, followed by the implementation of regression model and smoothing algorithm that ensure the stability and accuracy of the model.
- The developed methodology is demonstrated by simulations, based on vehicle test drives in order to illustrate the effect on the system performance.

978-1-6654-0976-6/21/$31.00 ©2021 IEEE

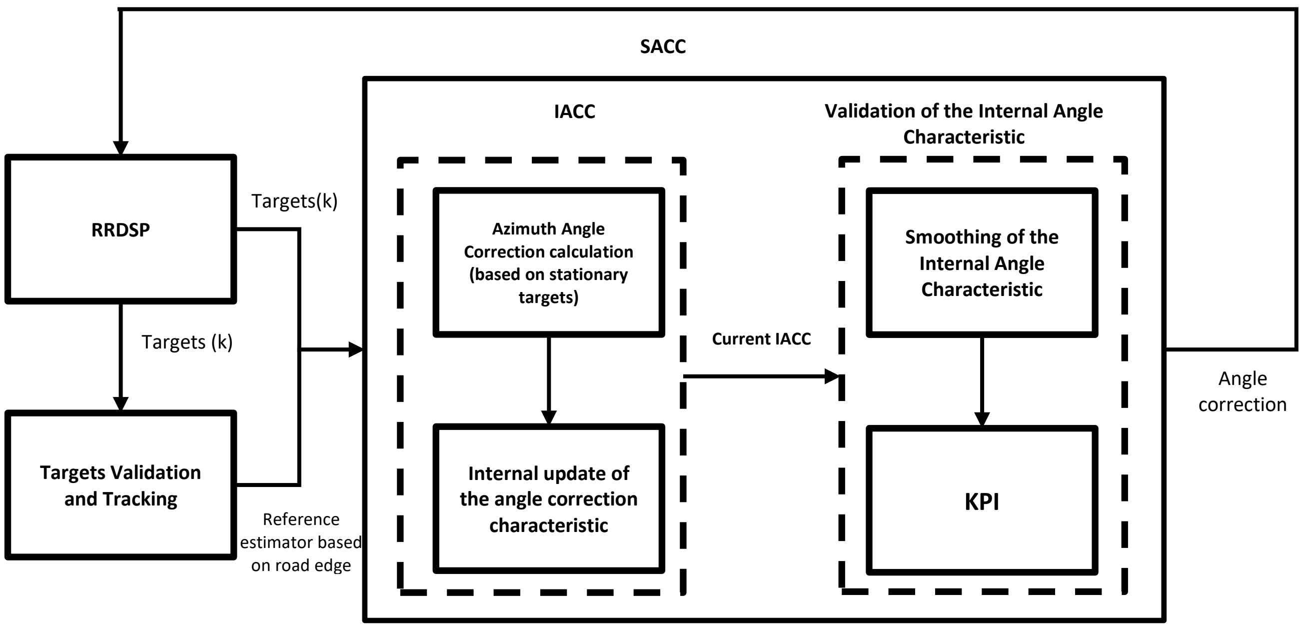

Fig. 1. Local offset compensation procedure.

The remainder of this paper is organized as follows: in Section II we introduce the general automatic calibration model. In Section III we analyze the automatic calibration process from the calculation of the reference angle based on stationary targets to the validation model and the KPIs (Key Performance Indicators) used. In Section IV we present the results obtained by simulating the presented algorithm using data gathered from a real test drive, provided by Hella KGaA Hueck & Co, followed by the conclusions in Section V.

II. The Methodology of The Automatic Calibration Model

The generation procedure of the azimuth angle correction characteristic is described in Fig.1. The System Angle Correction Characteristic (SACC) generator block receives as inputs the raw target list from the raw radar digital signal processing block (RRDSP) and a stationary structure consisting of the lateral position of the road edge, that will be used as the basis for the stationary reference calculation.

This raw target list, created in the current radar cycle k, that contains stationary targets, will be subjected to certain suitability criteria and the suitable targets will be used into the Azimuth Angle Correction calculation block.

The internal update of the angle correction characteristic is a process that takes multiple radar cycles to complete and will generate a plausible Internal Angle Correction Characteristic (IACC) using a combination of least squares regression and exponential moving average. Every correction of the IACC will then undergo a smoothing process, generating a smoothed angle characteristic that will be the basis for the SACC calculation. The new SACC will then be used by RRDSP in cycle k+1.

Besides the update of the SACC, the validation block also generates a series of KPIs that allow us to determine a general state of the current SACC.

III. Correction Calculation

To obtain a stable model, the processing flow requires activation conditions such as a straight drive and minimum ego velocity that will ensure a good target detection.

The stationary reference estimation along with the azimuth angle correction calculation and the update of IACC are described in Section III-A. The validation process is introduced in Section III-B and in Section III-C we define the KPIs based on the validation results.

A. Reference angle and update angle calculation

The SACC generator receives stationary targets, and the measured azimuth angle of each target $\tilde{\alpha}$ is a result of the azimuth angle of arrival α, affected by its systematic local offset $\Delta_{\alpha_{sys}}(\alpha)$ and Gaussian noise η_α, as shown in (1):

$$\tilde{\alpha} = \alpha + \Delta_{\alpha_{sys}}(\alpha) + \eta_\alpha \quad (1)$$

Thus, the true value of the azimuth angle is described in (2) in the following way:

$$\alpha = \tilde{\alpha} - \Delta_{\alpha_{sys}}(\alpha) - \eta_\alpha \quad (2)$$

The proposed method for providing an estimator for the azimuth angle α is presented in Fig. 2.

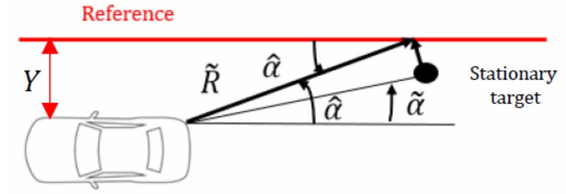

Fig. 2. Estimator of the azimuth angle of a target.

The principle behind our proposal of obtaining an estimator of the azimuth angle α of a stationary target is that if the target is close to a stationary reference structure, like the edge of the road (e.g. metal guardrail), then that target is a reflection from that structure and a shift in its lateral position is needed in order to obtain an accurate position. A stationary target with measured range $\tilde{R}$ and measured azimuth angle $\tilde{\alpha}$ that belongs to such reference Y has an estimated azimuth angle of:

$$\hat{\alpha} = \alpha + \eta_\alpha = \arcsin\left(\frac{Y}{\tilde{R}}\right) \quad (3)$$

However, it is possible that the value of the road edge lateral position is not stable from one radar cycle to another and that could cause wrong target assignments to the road edge, resulting in a poor estimation of the azimuth angle. The solution we propose includes modeling Y as a Gaussian random variable and a pre-calculation of the mean reference position over a number of N_{ref} radar cycles, based on the lateral position of the edge of the road, followed by a validation process that includes checking for the variance of the estimator. If the validation passes, over a maximum of M_{ref} radar cycles or until the variance condition is no longer fulfilled, the reference will still be updated, and suitable raw targets will be used for updating the IACC. Equation (4) describes the reference estimation process:

$$\hat{Y}_k = \frac{1}{k}\sum_i^k y_i, \quad (4)$$

where y_i is the precalculated reference, k is the current reference update cycle, with $N_{ref} < k \leq (N_{ref} + M_{ref})$.

Thus, (3) becomes:

$$\hat{\alpha} = \alpha + \eta_\alpha = \begin{cases} \arcsin\left(\frac{\hat{Y}_k}{\tilde{R}}\right), for\ \alpha \in [-\frac{\pi}{2}, \frac{\pi}{2}] \\ \pi - \arcsin\left(\frac{\hat{Y}_k}{\tilde{R}}\right),\ for\ \alpha \in (\frac{\pi}{2}, \pi] \\ -\pi - \arcsin\left(\frac{\hat{Y}_k}{\tilde{R}}\right),\ for\ \alpha \in [-\pi, -\frac{\pi}{2}) \end{cases} \quad (5)$$

The estimated difference angle is:

$$\alpha_{diff} = \hat{\alpha} - \left(\tilde{\alpha} + SACC(\tilde{\alpha})\right) \quad (6)$$

where $\left(\tilde{\alpha} + SACC(\tilde{\alpha})\right)$ represents the measured azimuth angle of the target, corrected with the latest azimuth correction provided by the SACC. In this way, the assignment angle is:

$$\alpha_{assignment} = \hat{\alpha} - SACC(\tilde{\alpha}) \quad (7)$$

In (6) and (7) we observe that the process of updating the IACC is based on the latest existing values of SACC in order to have a continuous correction updating process, in which the purpose of the IACC is to fine tune the SACC.

The pair consisting of α_{diff} and $\alpha_{assignment}$ will be sent to the IACC update block. The IACC and SACC have a structure similar to a table, as shown in Fig. 3. They have a starting angle α_{start}, a number of points and a minimum difference between neighbouring points α_{step}.

The next step is to find the index i of the nearest left neighbour of $\alpha_{assignment}$, as shown in (8).

$$i = \left[\frac{\alpha_{assignment} - \alpha_{start}}{\alpha_{step}}\right] \quad (8)$$

Both the left and right side corrections, associated with i and i+1 will be updated using the linear least squares fitting method, generating a slope and an intercept based on α_{diff}, $\alpha_{assignment}$ and a number of left and right neighbouring pairs of (α, SACC(α)). Thus, the associated left neighbour internal correction will be:

$$\alpha_{diff}(i) = m \cdot \left(\alpha_{start} + i \cdot \alpha_{step}\right) + n\ , \quad (9)$$

where m and n are the slope and the intercept resulted from applying the least squares fitting method [6].

Finally, from (5) and (6) we can observe that the obtained difference angle is corrupted by noise. In order to minimize the noise influence, the last step of updating the IACC for the given index i is based on an exponential moving average method [7], described in (10), using the filtering factor f:

$$IACC_{current}(i) = IACC_{previous}(i) + \ f \cdot (\alpha_{diff}(i) - IACC_{previous}(i)) \quad (10)$$

B. Validation model

After a number of N updates of the IACC have taken place, denoted as plausibility cycles, the next step before updating the SACC is to apply a smoothing process over the current IACC, resulting in a smoothed IACC. Our proposal of the smoothing mechanism is based on using a quality measure of the IACC updates of every supporting point as weights and the resulted smoothed correction for the supporting point k is calculated based on the neighboring corrections and their quality measures, as shown in (11):

$$SIACC(k) = \frac{\sum_{k-2}^{k+2} IACC(k)\frac{1}{\varepsilon_{Nk}}}{\sum_{k-2}^{k+2}\frac{1}{\varepsilon_{Nk}}}, \quad (11)$$

where SIACC (Smoothed IACC) is the resulting IACC after the smoothing process, N is the number of updates for the supporting point in the current update cycle and ε_{Nk} is the chosen quality measure of the updates.

For the quality measure, we have chosen an exponential moving average based standard error, presented in (12):

$$\varepsilon_{Nk} = \sqrt{\frac{\sum_{j=1}^{N}\left(\alpha_{diff_j}(k)\right)^2 - (N \cdot IACC(k)^2)}{N^2 - N}} \quad (12)$$

The new SIACC value for supporting point k will be added to the last SACC value. To avoid angular ambiguities introduced by the SACC, we propose recalculating the SACC neighbors, k-1, and k+1 using a simple linear regression. Finally, the new SACC value for supporting point k is:

$$SACC(k) = \frac{SACC(k-1) + SACC(k+1)}{2} \quad (13)$$

C. Key performance indicators

During the lifetime of the vehicle, the driving scenarios are as diverse as the driving environment. However, the SACC behavior must at the same time be stable and robust, but it also must be accurate and easily adaptable for the whole lifetime of the sensor, while also considering the sensor aging and any possible scenarios where the cover or bumper might be hit.

For this, we propose the usage of a global coefficient of variance that encapsulates the overall stability and robustness of the SACC. Firstly, we calculate the local variance based on the IACC latest updates, as shown in (14):

$$\sigma_{IACC(k)}{}^{2} = \frac{\sum_{j=1}^{N}\left(\alpha_{diff_j}(i)\right)^{2} - \frac{1}{N}\left(\sum_{j=1}^{N}\alpha_{diff_j}(i)\right)^{2}}{N-1} \quad (14)$$

The overall variance coefficient is calculated using an exponential moving average filter of factor f_{σ^2}:

$$\sigma_{current}{}^{2} = \sigma_{previous}{}^{2} + f_{\sigma^2} \cdot (\sigma_{new}{}^{2} - \sigma_{previous}{}^{2}) \quad (15)$$

The convergence of the SACC can be described in terms of the absolute value of all smoothed differences, $SIACC$, between the measured azimuth and assumed references. The remaining offset, θ is expressed in (16) based on an exponential moving average filter of factor f_{θ} :

$$\theta_{current} = \theta_{previous} + f_{\theta} \cdot (\theta_{new} - \theta_{previous}) \quad (16)$$

Finally, a sense of SACC progress can be expressed as a function of θ, as shown in (17):

$$\rho_{SACC} = \begin{cases} \frac{\theta_{min}}{\theta_{current}} \cdot 100\ [\%], \theta_{current} > \theta_{min}, \\ 100\%,\ otherwise \end{cases} \quad (17)$$

where ρ is the current SACC progress.

IV. Numerical Results

The simulation results for the proposed method are presented in this section. These results are based on the methodology described in Section II along with the correction calculation method described in Section III. The results are based on real data from a test drive effectuated on a highway, in optimal driving and environmental conditions for both rear and front radar sensors. This data is used as input for our simulation environment.

TABLE I. Angle Correction Curve Calculation Parameters

Parameter	Symbol	Value
Minimum vehicle velocity	-	5 m/s
Maximum vehicle yaw rate	-	0.5 deg/s
Number of road edge measurements	N_{ref}	35
Number of road edge target updates	M_{ref}	35
Maximum reference standard deviation	-	1 m
Target filter factor for EMA update	f	0.5
Number of plausibility cycles	N	30
Number of points used for least squared method	-	9
Maximum target distance from reference	-	2 m
Minimum target SNR	-	15 dB
Maximum error	1	deg
Maximum standard deviation	1	deg
EMA Variance coefficient	f_{σ^2}	0.01
EMA Remaining Angle Offset coefficient	f_{θ}	0.01
Remaining offset Angle for 100% progress	θ_{min}	0.5 deg

In Table I are presented the parameters used for enabling the angle correction curve calculation functionality and for the correction calculation.

Fig. 3 illustrates the calculated SACC, represented with blue, for all sensors compared to their reference SACC values, represented with red. Fig. 4. shows the absolute error between the measured SACC and the reference SACC. The error is higher at the two extremities of the measured azimuth angle interval ([-34, 20] deg and [100-126] deg intervals), mainly due to the lack of suitable radar raw targets around edge of the sensor's field of view. This is also enforced by the data shown in Fig. 5, where the histogram of updates is presented. Moreover, from Fig. 3 we can also observe that within the angular area of 80-100 deg the absolute error is very high compared to the rest of the interval. This is mainly due to the uncertainty of (5) around the angles close to 90 deg.

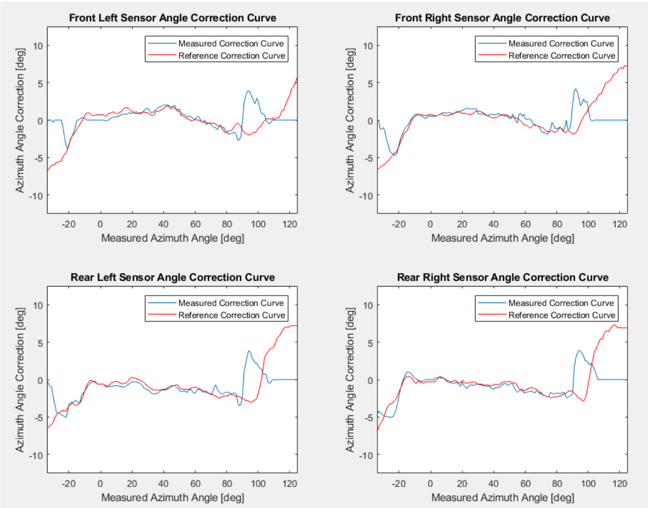

Fig. 3. Comparison of the measured SACC against the reference SACC.

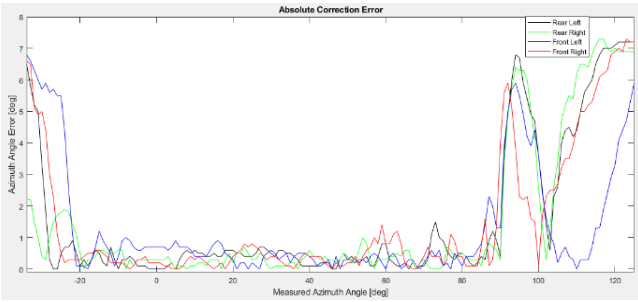

Fig. 4. Absolute SACC error.

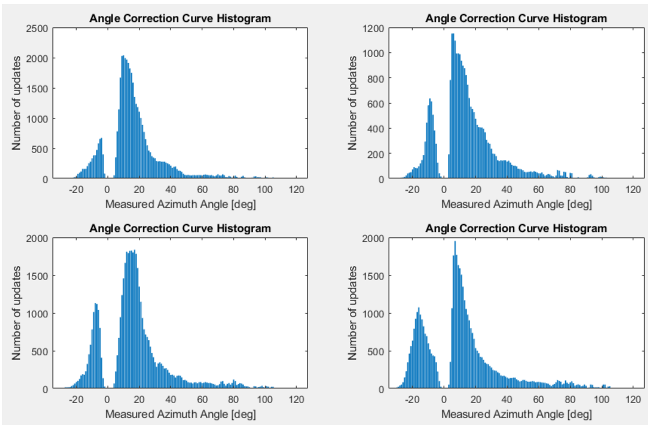

Fig. 5. SACC Histogram.

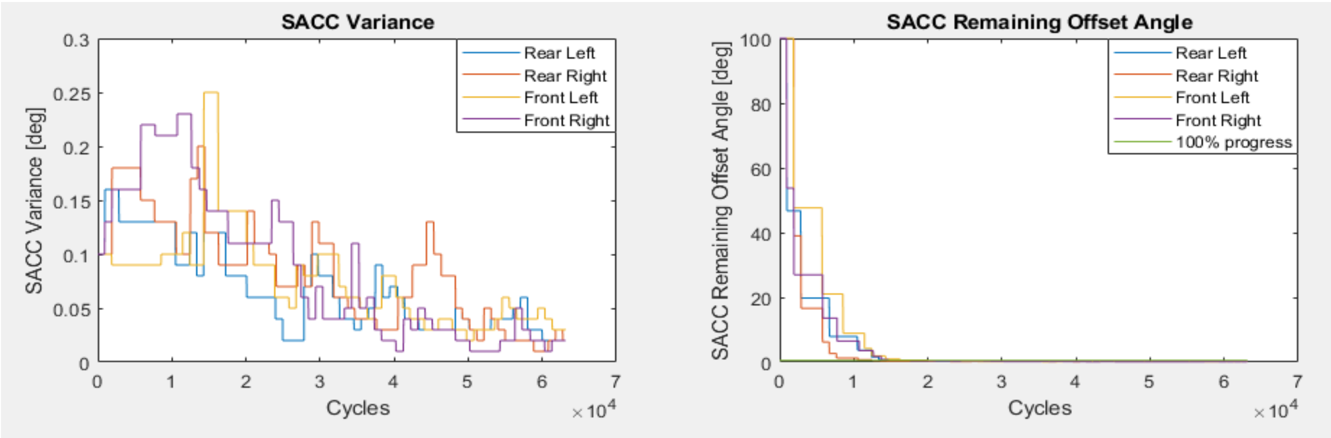

Fig. 6. SACC statistics.

In Fig. 6. are presented the statistics of the SACC, defined as the variance and the remaining offset angle as a function of radar cycles. It can be noted that the SACC variance rises in the beginning, then remains at a certain level, according to the environment and then will experience short term changes in value in case of changing the environment. The other SACC statistic, the remaining offset, is maximal at the start of the adaptation process and it will lessen over time to a certain minimal threshold, reaching a convergence point.

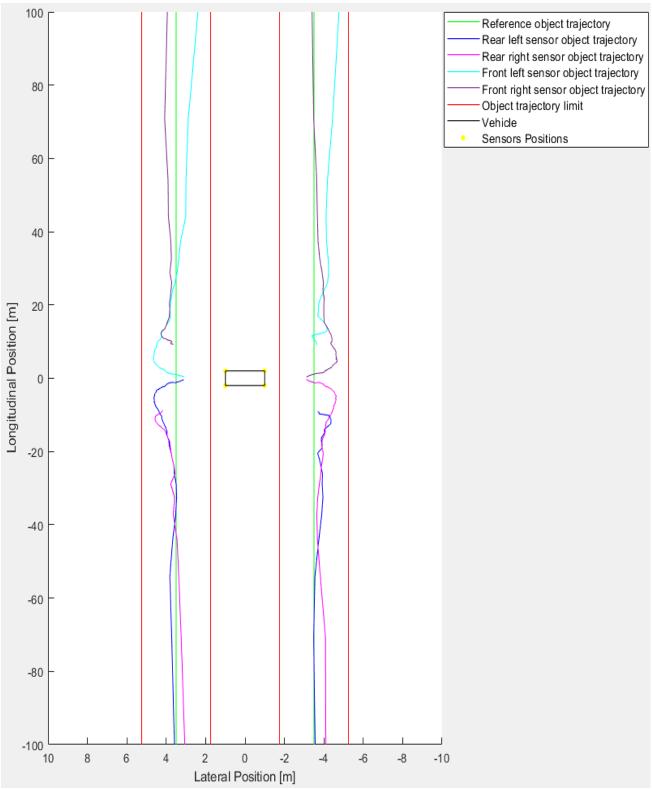

Fig. 7. Overtaking objects scenario.

Finally, in Fig. 7, we present a simulation of a specific scenario where different objects are performing overtaking maneuvers on adjacent lanes in the SACC angular intervals. The green lines represent the ideal trajectory followed by the center of an object created by the targets corrected by the reference SACC. The red lines are described as the maximum lateral position deviation of the center of the overtaking object.

The meaning of these limits is that we can consider a radar lane assignment error of an object if more than half of the object width is detected on the wrong lane. In our scenario, a wrong assignment is considered if the sensors' trajectories intersect with the limit trajectory in the given longitudinal interval. Considering a lane width of 3.5 m, we placed our vehicle on the middle of the central lane and the center of the overtaking objects on the middle of the adjacent lanes. That means that the lateral positions of the limits are at ± 1.75m and ± 5.25m. We can observe from Fig. 7, that the trajectory of the objects generated from targets corrected by the proposed method, satisfy the requirements for a correct lane assignment in the adjacent lanes. However, we can observe that at high angles, the objects' trajectories are close to the ± 5.25m limit.

V. CONCLUSIONS

In this paper, a novel autocalibration method was introduced for performing a continuously adjustable and tunable azimuth automatic calibration process which can adapt any vehicle, can accurately compensate azimuth local offsets in a robust manner in the [-20,80] degrees interval and can provide statistical data that characterize the resulting angle correction curve. The method was proven on simulations based on real test drive data, demonstrating the effect on the system performance.

ACKNOWLEDGMENT

The authors would like to thank Hella KGaA Hueck & Co for providing the drive test data and for the overall support.

REFERENCES

[1] F. Pfeiffer and E. M. Biebl, "Inductive compensation of high-permittivity coatings on automobile long-range radar radomes," IEEE T Microw Theory, vol. 57, no. 11, pp. 2627–2632, 2009

[2] I. Gupta and A. Ksienski, "Effect of mutual coupling on the performance of adaptive arrays," IEEE T Antenn Propag, vol. 31, no. 5, pp. 785–791, Sep 1983

[3] M. Harter, J. Hildebrandt, A. Ziroff, and T. Zwick, "Self-Calibration of a 3-D-Digital Beamforming Radar System for Automotive

Applications with Installation Behind Automotive Covers," IEEE T Microw Theory, vol. 64, no. 9, pp. 1–7, 2016.

[4] K. Suzuki, C.Yamano, and Y. Miyake, "Bias angle error self-correction for automotive applications using phased array radars installed behind bumpers," IEEE MTT-S International Conference on Microwaves for Intelligent Mobility (2017).

[5] S. Kostka, Y. Zhou, and E. Warsitz, "Verfahren zur Kompensation von Winkelmessfehlern," 2013, DE102013203574A1.

[6] F. M. Dekking, A Modern Introduction to Probability and Statistics, U.K., London:Springer-Verlag, 2005.

[7] F. Klinker, "Exponential moving average versus moving exponential average", Math Semesterber 58, 97–107 (2011).